HHS Public Access

Author manuscript

J Immunol. Author manuscript; available in PMC 2018 February 15.

Published in final edited form as:

J Immunol. 2017 February 15; 198(4): 1660–1672. doi:10.4049/jimmunol.1601495.

Inactivation of Rab11a GTPase in macrophages facilitates phagocytosis of apoptotic neutrophils

Chunling Jiang[*,‡], **Zheng Liu**[*,‖], **Rong Hu**[#], **Lulong Bo**[*,‖], **Richard D. Minshall**[*,†], **Asrar B. Malik**[†], and **Guochang Hu**[*,†]

[*]Department of Anesthesiology, University of Illinois College of Medicine, Chicago, IL 60612

[†]Department of Pharmacology, University of Illinois College of Medicine, Chicago, IL 60612

[#]Washington University in St Louis, St Louis, MO 63130

[‡]Department of Anesthesiology, West China Hospital, Sichuan University, Chengdu, Sichuan 610041, China

[‖]Department of Anesthesiology and Intensive Care, Changhai Hospital, Shanghai 200433, China

Abstract

The timely and efficient clearance of apoptotic neutrophils by macrophages (efferocytosis) is required for the resolution of inflammation and tissue repair, but the regulatory mechanisms remain unclear. Here, we investigated the role of the small GTPase Rab11a in regulating efferocytosis, and on this basis the resolution of inflammatory lung injury. We observed that apoptotic neutrophil feeding induced a rapid loss of Rab11a activity in bone marrow-derived macrophages and found that depletion of Rab11a in macrophages by siRNA dramatically increased the phagocytosis of apoptotic neutrophils compared with control cells. In addition, overexpression of wild type Rab11a inhibited macrophage efferocytosis, whereas overexpression of dominant negative Rab11a (Rab11a S25N) increased the clearance of apoptotic neutrophils. Rab11a knockdown also increased the surface level of CD36 in macrophages, but reduced cell surface expression of a disintegrin and metalloproteinase (ADAM) 17. Depletion of ADAM17 rescued the decreased surface CD36 expression found in macrophages over-expressing wild type Rab11a. Also, blockade of CD36 abolished the augmented efferocytosis seen in Rab11a-depleted macrophages. In mice challenged with endotoxin, intratracheal instillation of Rab11a-depleted macrophages reduced neutrophil count in bronchoalveolar lavage fluid, increased the number of macrophages containing apoptotic neutrophils, and prevented inflammatory lung injury. Thus, Rab11a inactivation in macrophages as result of apoptotic cell binding initiates phagocytosis of apoptotic neutrophils via the modulation of ADAM17-mediated CD36 cell surface expression. Our results raise the possibility that inhibition of Rab11a activity in macrophages is a promising strategy for activating the resolution of inflammatory lung injury.

Correspondence should be addressed to: Guochang Hu, M.D., Ph.D., 3200W UICH, MC 515, Department of Anesthesiology, University of Illinois, College of Medicine, 1740 W. Taylor St. Chicago, IL 60612-7239, USA, Phone: (312) 996-4692, Fax: (312) 996-1225, gchu@uic.edu.

Disclosures: The authors have no financial conflict of interest.

Introduction

Acute inflammation is the survival response of a host against invading pathogenic microorganisms and it is characterized by rapid emigration of polymorphonuclear neutrophils (PMNs) from blood vessels to sites of infection. The recruited PMNs are required for the neutralization and removal of microbes but can also cause significant damage to host tissues if the acute inflammatory response is uncontrolled and excessive (1). Thus, efficient resolution of inflammation depends on not only cessation of PMN infiltration but also the recruitment and differentiation of macrophages, which remove the spent pro-inflammatory PMNs and tissue debris to restore tissue homeostasis (2). After tissue injury, recruited PMNs undergo apoptosis and are subsequently phagocytized by macrophages via a process termed efferocytosis. Efferocytosis by macrophages is critical for tissue remodeling, modulation of immune responses, and resolution of inflammation (3). Clearance of apoptotic PMNs initiates a phenotype switch from M1 to M2 macrophages, which secrete anti-inflammatory cytokines, such as TGF-β and IL-10, that in turn inhibits the release of inflammatory cytokines such as TNF-α and IL-6 (4,5). Efferocytosis by a set of macrophages also triggers the production of specialized pro-resolving mediators (e.g. resolvins and lipoxins) that signal the restoration of vascular integrity and regeneration of injured tissues (6).

Efferocytosis is a coordinately orchestrated process involving the recruitment of macrophages to inflammatory sites, recognition of the marked apoptotic cells, engulfment, and ultimately removal of apoptotic cells (7). An essential recognition or “find-me” signal is the plasma membrane inner leaflet phospholipid phosphatidylserine (PS) localized on the outer surface of apoptotic cells and additional signals include the release of chemokines and lysophosphatidylserine by apoptotic cells, which induces macrophage recruitment (5,7). In response, the macrophage increases the expression of bridge molecules and cell surface receptors that act as tethers for the “catch me” step (3,7). This then proceeds to the “eat me” step when the macrophage engulfs apoptotic cells through generation of large phagosomes (a.k.a efferosomes) to degrade the ingested cells (3,7). Recognition and binding of apoptotic cells by receptors on the macrophage surface is thus a key event for macrophage recruitment and efferocytosis (8,9). Some efferocytosis receptors that directly recognize PS include brain-specific angiogenesis inhibitor-1 (BAI-1), stabilin 1 and 2, and members of the T-cell immunoglobulin mucin domain protein family (TIM) (3,10). Also, other efferocytosis receptors can indirectly recognize PS via interaction with specific bridging molecules in the serum or produced by macrophages themselves; these receptors include integrins $\alpha_v\beta_3$/$\alpha_v\beta_5$, CD36 and Tyro3/Axl/Mer (TAM), each of which recognizes the bridging molecules milk-fat-globule-epidermal growth factor 8 (MFG-E8/lactaherin), thrombospondin-1, and protein S/growth arrest-specific gene 6 (Gas6) respectively (3,10,11).

Rab (Ras-related proteins in brain) GTPases, the largest subfamily of the Ras superfamily of small G-proteins, serve as master regulators of intracellular membrane trafficking including cargo selection, vesicle budding, moving, tethering, docking, and targeting (12,13). Based on distinct subfamily-specific sequence motifs, Rab proteins are grouped into approximately 70 subfamilies. In particular, the Rab11 subfamily members Rab11a, Rab11b, and Rab25 are shown to be central regulators of endocytic membrane recycling in both polarized and non-

polarized cells (14). Rab11a is among the most prominent recycling endosome components and plays important roles in broader intracellular domains, encompassing the trans-Golgi network, post-Golgi secretory vesicles, and the recycling endosome (15-17). Interestingly, Rab11a has also been reported to be involved in macrophage phagocytosis, and Rab11a activation induced FcγR-mediated internalization of IgG-opsonized particles (18). Thus, we addressed the possibility that Rab11a is essential for regulating phagocytosis of apoptotic PMNs by macrophages, thereby mediating resolution of inflammation.

We found that Rab11a inactivation enhanced macrophage efferocytosis and consequently the resolution of lung inflammation and injury via inhibiting translocation of a disintegrin and metalloproteinase (ADAM) 17 from the cytoplasm to the cell surface, which prevented cleavage of surface CD36 on macrophages. Our results showed that inhibition of Rab11a activation in macrophages may be a promising strategy for the resolution of inflammatory lung injury through the effective clearance of dying PMNs.

Materials and Methods

Reagents

LPS (*E. Coli*. O55:B5, L2880) was from Sigma-Aldrich. Anti-Rab11a (#2413), Na^+/K^+ ATPase (#3010) and GAPDH (#2118) Abs were from Cell Signaling. Anti-HRP–conjugated Abs were obtained from Santa Cruz Biotechnology. Anti-CD36 (ab23680, ab133625) Abs, anti-ADAM17 (ab57484, ab39163) Abs and myeloperoxidase (MPO) assay kit were ordered from Abcam. Cytokine ELISA kits were purchased from Biolegend. Rab11a and ADAM17 siRNAs were from Dharmacon. CellTracker™ Green and Red, pHrodo succinimidyl ester (pHrodo-SE), Alexa fluor 594 or 488-conjugated Abs, Lipofectamine 2000, Lipofectamine RNAiMAX transfection reagent, Mem-PER™ Plus Membrane Protein Extraction Kit, BSA, FBS, and heat-inactivated FBS were from Invitrogen. Rab11 activation assay kit was from Neweast Bioscience. Radioimmunoprecipitation assay (RIPA) buffer was from Pierce Biotechnology. Bicinchoninic acid kits and sample buffer were from Bio-Rad. DMEM/ F12 and nonenzymatic cell dissociation solution were from Cellgro. Wild type Rab11a and dominant negative mutant Rab11a S25N plasmids were a gift from Dr. Wei Guo (University of Pennsylvania, Philadelphia, PA).

Mice

C57BL/6J male mice (25–30 g, 8-12 wk) obtained from The Jackson Laboratory (Bar Harbor) were inbred in microisolator cages under specific pathogen-free conditions, fed with autoclaved food. All animal procedures were approved by the Institutional Animal Care and Use Committee prior to execution. All studies were performed under anesthesia using either 1-3% isoflurane (inhalation) or ketamine (90 mg/kg, i.p.).

Cell culture

J774A.1 murine macrophages (American Type Culture Collection) were cultured in DMEM supplemented with 10% FBS at 37°C in CO_2 (5%, v/v) incubator. The cells were washed three times in PBS to remove media and non-adherent cells prior to transfection. The cells between passages 4–10 were used throughout this study.

Isolation and culture of mouse bone marrow–derived macrophages

Murine bone marrow–derived macrophages (BMDMs) were isolated as described (19). In brief, mice were sacrificed by rapid cervical dislocation. Bone marrow was flushed from femurs and tibias with 2 to 5 ml of PBS (without Ca^{2+} and Mg^{2+}). Collected bone marrow cell suspensions were centrifuged for 10 min at 500 × g at room temperature. Cell pellets were then resuspended in macrophage complete medium (DMEM/F12 with 10% FBS, 20% L-929 cells conditioned medium, 10 mM L-glutamine, 100 IU/ml penicillin, and 100 mg/ml streptomycin). Cells (4×10^5) were then added to each sterile plastic petri dish in 10 ml macrophage complete medium and incubated at 37°C and 5% CO_2. On d 3, another 5 ml macrophage complete medium was added to each dish. The adherent cells after 7 d in culture were >95% pure macrophages, as assessed by the expression of cell-surface markers HLA-DR, CD11b, and CD206, and these BMDMs were used for all relevant experiments.

Isolation of PMNs and induction of apoptosis

PMNs were isolated from mouse peripheral blood by density-gradient Ficoll-Histopaque as described previously (20). Apoptosis of PMNs was induced by the exposure of cells to UV irradiation (254 nm, UVS-26, 6W bulb 0.02 $J{\cdot}s^{-1}{\cdot}cm^{-2}$) for 15 min and then incubation for 3 h in a CO_2 (5% , v/v) incubator at 37°C. Approximately 91% of PMNs in this study were apoptotic as verified by annexin V^+ cells using flow cytometric analysis.

Phagocytosis of IgG-opsonized latex beads

FITC-conjugated polystyrene latex beads covalently were opsonized with mouse IgG1 (Sigma-Aldrich) to study the FcγR-mediated phagocytosis. In brief, latex beads (diameter, 1.0 μm) were washed three times and then incubated in HBSS containing 3 mg/ml of mouse IgG1 at 4 °C on a rotator for 8 h to allow sufficient binding. After incubation, the beads were resuspended and washed three times with cold HBSS to remove any unbound IgG1. Macrophages (10^6/well, seeded in 6-well plates) were incubated with IgG1-opsonized beads at a ratio of 10 beads per cell at 37°C for 20 min, washed with ice-cold HBSS, fixed in 4% paraformaldehyde. Phagocytosis was visualized by a DS-Fi2 fluorescence microscope (Nikon) and images were captured using a Nikon DS-U3 camera. The phagocytic index was calculated using the following formula: phagocytic index = number of latex beads internalized by 100 macrophages counted in 10 random fields (21).

Macrophage efferocytosis assay *in vitro*

Apoptotic PMNs ($2\text{-}3\times10^7$/ml) were labeled by incubation of cells with CellTracker™ Red at 37°C for 15 min, while mouse BMDMs or J774 macrophages were seeded in a 24-well plate and incubated with CellTracker™ Green for 15 min. Macrophages were then overlaid with apoptotic PMNs (1:10 ratio) for 2 h. After vigorous washing with PBS, the macrophages engulfing labeled apoptotic PMNs were analyzed using fluorescence microscopy. Phagocytic activity was expressed as phagocytic index, calculated as the percentage of macrophages containing at least one ingested PMN.

Assay of efferocytosis by alveolar macrophages *in vivo*

Bronchoalveolar lavage (BAL) was performed by intratracheal injection of 1 ml PBS followed by gentle aspiration. The lavage was repeated three times. The pooled BAL fluid was centrifuged, and cell pellets were suspended in PBS. Cell suspensions were cytospun onto slides with a cytocentrifuge (Shandon). Slides were stained with Diff-Quick dye (Dade Behring) and examined at magnifications of 20× and 40× by light microscopy. A minimum of 300 macrophages were scored for each sample. Phagocytosis was expressed as the percentage of macrophages ingesting apoptotic cells and apoptotic bodies (22).

The phagocytosis of apoptotic PMNs by alveolar macrophages *in vivo* was carried out by intratracheal instillation of exogenous mouse apoptotic PMNs labeled with the pH-sensitive fluorescent dye pHrodo™ Red-SE (20 ng/ml) at room temperature for 30 min. pHrodo™ Red-SE-labeled apoptotic PMNs (1.0×10^7 in 100 μl) was intratracheally instilled 2 d following CellTracker™ Green-labeled BMDM (2.0×10^6) transplantation. After 3 h of PMN instillation, BAL was performed. Cells in BAL fluid were washed, resuspended and analyzed by flow cytometry (23). pHrodo-SE was chosen to allow the detection of only ingested apoptotic PMNs, due to increased light emission in the acidic environment of the phagosomes of phagocytes. Attached apoptotic PMNs were excluded since pHrodo-SE was nonfluorescent at neutral pH (24).

Rab11a and ADAM17 knockdown in macrophages

J774A.1 macrophages or BMDMs grown in 6-well plates were transfected at 50–70% confluence with 50 nM Rab11a small interfering (si) RNA, ADAM17 siRNA, or non-targeting control siRNA (Dharmacon) according to the protocol provided by the manufacturer. Successful knockdown of Rab11a or ADAM17 in macrophages was confirmed by Western blot analysis. All experiments were performed 48 h posttransfection.

Rab11a cDNA transfection

J774A.1 macrophages were transfected with pcDNA6 plasmid vector containing cDNAs of GFP-tagged wild type Rab11a or dominant negative mutant Rab11a S25N. Macrophages were incubated with a mixture of 4 μg cDNA and 10 μl Lipofectamine 2000 (Invitrogen) in each well of a six-well plate. At 48 h posttransfection, successful expression of exogenous Rab11a was confirmed by Western blot analysis of cell lysates.

Flow cytometry

For analysis of PMN apoptosis, PMN suspensions were centrifuged for 5 min at 400 × g and washed twice with cold PBS (without Ca^{2+}/Mg^{2+}) containing 1% BSA. The pellets were resuspended in ice-cold PBS (without Ca^{2+}/Mg^{2+}) with 1% BSA at a final cell concentration of 2×10^7/ml. PMNs were incubated with FITC-conjugated annexin V (BD Biosciences) and propidium iodide for 45 min on ice, washed, and analyzed by flow cytometry (Becton Dickinson LSR II). Early apoptotic PMNs were defined as those annexin V^+/ propidium $iodide^-$, and necrotic PMNs as propidium $iodide^+$ nonpermeabilized cells. For analyzing surface expression of CD36 and ADAM17, cell suspensions were centrifuged for 5 min at 200 × g and washed twice with cold PBS (without Ca^{2+}/Mg^{2+}) with 1% BSA. Nonspecific Ab-binding sites were blocked by incubation in PBS containing 10% goat serum and 0.3 M

glycine for 30 min at room temperature. Cells were then incubated with anti-CD36, anti-ADAM17 Ab or isotype control Ab for another 30 min at room temperature. After washing, cells were stained with Alexa Fluor 594-conjugated goat anti-mouse or anti-rabbit IgG secondary Ab fluorescein for 30 min at room temperature, washed, and subjected to flow cytometric analysis.

Rab11a-GTP pull-down assay

Rab11a pull-down assay was performed using Rab11 activation assay kit (Neweast Bioscience) according to the manufacturer's instructions (17). Cells were washed once with ice-cold PBS and lysed with cell lysis buffer. Lysates were centrifuged at 13,000 × g for 10 min, and the supernatant was incubated with 1.0 μg anti-active Rab11 Ab coupled with protein A/G agarose. The reaction mixture was gently rocked for 1 h at 4°C. The beads were then collected by centrifugation at 5000 × g, incubated at 4°C for 1 min, and washed twice with lysis buffer. Beads were finally resuspended in Laemmli sample buffer (30 μl) and boiled for immunoblotting with anti-Rab11a Ab. The total level of Rab11a was measured by Western blot analysis of cell lysates.

Immunofluorescence

Immunofluorescence was performed as described previously with slight modifications (19). Briefly, cells plated on coverslips were fixed with 4% paraformaldehyde for 10 min, washed 3 times with PBS for 10 min, permeabilized with 0.2% Triton X-100 in PBS for 5 min, incubated with anti-Rab11a, anti-CD36 or anti-ADAM17 (1:100) Ab at 4°C overnight, followed by incubation with Alexa Fluor 594– or Alexa Fluor 488–conjugated secondary Abs (1:1000) for 1 h. Cell nuclei were stained with DAPI (5 μg/ml) for 10 min. The cells were rinsed three times and finally mounted on glass slides using ProLong antifade mounting medium (Molecular Probes). Confocal images were acquired with a laser-scanning confocal microscope (Zeiss LSM 510 META) using Hg lamp and UV-filter set to detect DAPI (band pass 385–470 nm emission), 488 nm excitation laser line to Alexa 488 (band pass 505–550 nm emission), and 568 nm excitation laser line to Alexa Fluor 594 (excitation/emission ~590/617 nm). Optical sections had a thickness of 1 mm (pinhole set to 1 Airy unit).

Western blotting and immunoprecipitation

Cells were lysed by radio immunoprecipitation assay (RIPA) buffer supplemented with 1 mM PMSF, 1 mM Na_4VO_3, protease, and phosphatase inhibitor mixture. Membrane Protein Extraction Kit was utilized to extract membrane proteins from cells. The cell lysates were sonicated for 10 s and centrifuged at 10,000 × g for 10 min at 4°C. Protein concentration was measured using a Bio-Rad protein assay kit (Bio-Rad Laboratories). The samples were subjected to PAGE (10–12%) and the separated proteins were transferred onto nitrocellulose membranes (Invitrogen). The membranes were blocked with 5% nonfat milk, probed with primary Abs overnight at 4°C, and then incubated with HRP-conjugated secondary Abs (1:3000~5000) at room temperature for 1 h. The protein bands were detected with Odyssey Fc Imager (LI-COR Biosciences). Relative band densities of the various proteins were measured from scanned films using ImageJ Software (NIH).

Immunoprecipitation analysis was conducted as described previously (17,19). Cell lysates were precleared with 1 μg normal rabbit IgG and 20 μl protein A+G agarose beads for 2 h at 4°C and then incubated overnight at 4°C with primary Ab, followed by addition of 25 μl Protein A/G PLUS-Agarose and further incubated at 4°C for 2 h. The samples were electrophoresed on SDS-PAGE gels (10–12%) and subsequently transferred to nitrocellulose membranes. The protein bands are detected with digital imaging equipment and analyzed with ImageJ Software.

Depletion of alveolar macrophages in mice

Depletion of alveolar macrophages was performed as described previously (19,25). The clodronate liposome (Encapsula NanoSciences LLC) was intratracheally delivered to the anesthetized mice with ketamine (90 mg/kg, i.p.). Lavageable alveolar macrophage count was reduced by 95 % at 2 d following clodronate liposome nebulization.

Murine model of LPS-induced acute lung injury and pulmonary macrophage transplantation

BMDMs were isolated and cultured as described above. BMDMs were transfected with a control siRNA or Rab11a siRNA. Alveolar macrophage-depleted mice were challenged with LPS (3.5 μg/kg, i.t.). At d 3 after LPS challenge, PBS or BMDMs transfected with a scrambled siRNA or Rab11a siRNA (2×10^6 cells, 200 ml total volume each) were given to alveolar macrophage-depleted mice via intratracheal instillation as described previously (26). Mice were sacrificed and lung injury was evaluated by analysis of BAL fluid, wet/dry lung weight ratio measurement, and biochemical/immunological analysis of lung tissue at different time points.

Lung tissue MPO activity

MPO activity in the lung as a marker of PMN sequestration was measured according to manufacturer's protocol (27). Briefly, lung tissue (~50 μg) was homogenized in 1 ml of cold sample buffer and centrifuged at 16,000 g for 30 min at 4°C. MPO activity was measured in 100 μl of supernatants in duplicate by using development reagent at 450 nm and expressed as change in absorbance per mg of protein.

Quantification of PMN infiltration in the lung

At the end of the experiments, BAL was performed to enumerate the absolute number of PMNs in the intra-alveolar inflammatory exudates as described previously (27). In brief, lungs were lavaged by an intratracheal injection of 1 ml PBS followed by gentle aspiration. The procedure was repeated three times. After the collected BAL fluid was centrifuged, cell pellets were suspended in PBS. Cell suspension (300 μl) was cytocentrifuged on to a glass slide at 300 rpm for 5 min with a cytocentrifuge (Shandon). Slides were stained with Diff-Quick dye (Dade Behring) and examined at magnifications of 20× and 40× by light microscopy. The percentage of PMNs was calculated after counting 300 cells in randomly selected fields.

Lung vascular injury and edema formation

BAL protein concentration was measured using a Bio-Rad protein assay kit (Bio-Rad Laboratories) to evaluate permeability of the alveolar-capillary barriers (27). At the end of experiments, lungs were weighed, dried, and reweighed. Wet-to-dry lung weight ratio was used as an index of lung water content and edema.

Lung histology and lung injury scoring

At the end of animal experiments, the lungs were fixed by instillation of 4% paraformaldehyde (Sigma-Aldrich) in PBS and held for 2 h under 25 cm H_2O pressure. The fixed lungs were washed with PBS and dehydrated in 70% ethanol before paraffin embedding. Lung tissue sections (4.0 μm) were stained with H&E.

The severity of lung injury was evaluated independently by two blinded investigators according to the histological semiquantitative scoring system as described previously (28). Each investigator scored all lung fields per slide at 20× magnification. Within each field, points were assigned on a scale from 1–5 for the following criteria: 1, normal; 2, focal (<50% lung section) interstitial congestion and inflammatory cell infiltration; 3, diffuse (> 50% lung section) interstitial congestion and inflammatory cell infiltration; 4, focal (< 50% lung section) consolidation and inflammatory cell infiltration; and 5, diffuse (> 50% lung section) consolidation and inflammatory cell infiltration. Injury scores were averaged for the two investigators. The mean score was used for comparison between groups.

Measurements of cytokine levels

The levels of TNF-α, IL-6, TGF-β1 and IL-10 in BAL were measured with commercial ELISA kits (Biolegend) according to the manufacturer's instructions. Each value represents the means of triplicate determinations.

Statistical analysis

One-way ANOVA and Student Newman–Keuls test for post hoc comparisons were used to test differences between control and experimental groups. The differences in phagocytosis of IgG-opsonized latex beads between groups were evaluated by a two-way ANOVA. Data are expressed as mean ± SEM. Differences were considered significant when $P < 0.05$.

Results

Depletion of Rab11a enhances macrophage phagocytosis of apoptotic PMNs

Rab11 was shown to be expressed in multiple intracellular compartments including phagosomes of macrophages. In murine peritoneal macrophages and the RAW cell line, Rab11 is required for FcγR-mediated phagocytosis (18), raising the possibility that Rab11a activation facilitates efferocytosis and is involved in subsequent resolution of inflammation. Therefore, first we genetically manipulated Rab11a expression in macrophages and examined its role in the phagocytosis of apoptotic PMNs. As shown in Figure 1A (left), Rab11a expression was reduced by >90% at 48 h posttransfection with a specific siRNA. Depletion of Rab11a in fact enhanced phagocytosis of apoptotic PMNs by J774A.1 macrophages compared to control cells (Fig. 1A). Consistently, in BMDMs, silencing of

Rab11a also induced engulfment of apoptotic PMNs (Fig. 1B). To validate the role of Rab11a in the FcγR-mediated phagocytosis, FITC-conjugated polystyrene latex beads were opsonized with mouse IgG1. We observed that Rab11a knockdown inhibited engulfment of IgG-opsonized beads compared to control siRNA. Approximately 80% of control cells contained 4 or more beads whereas > 40% of Rab11a-depleted macrophages had no beads and the overall distribution was shifted towards lower numbers (Fig. 1C). Thus, these results demonstrate that Rab11a is a negative regulator of macrophage efferocytosis.

Rab11a inactivation is required for clearance of apoptotic PMNs

Based on our finding that Rab11a inhibited the phagocytosis of apoptotic PMNs by macrophages, we next asked if GTP/GDP-dependent activity of Rab11a is required for the phagocytic clearance of apoptotic PMNs. Rab11a activity during efferocytosis was determined by the relative amount of GTP-bound Rab11a (active). As shown in Figure 2A, inclusion of apoptotic PMNs suppressed Rab11a activation in a time-dependent manner. At 15 min, GTP-Rab11a was almost completely lost (Fig. 2A). To elucidate the role of Rab11a activity in regulating phagocytosis of apoptotic PMNs, J774A.1 macrophages were transfected with GFP-tagged wild-type Rab11a or dominant negative Rab11a-S25N plasmid (Fig. 2B). Macrophages expressing wild-type Rab11a showed a decreased engulfment of apoptotic PMNs as compared to the vector control group. In contrast, overexpression of Rab11a-S25N dramatically augmented phagocytosis of apoptotic PMNs (Fig. 2C, 2D). Thus, Rab11a inactivation promotes macrophage phagocytosis of apoptotic PMNs.

Rab11a negatively regulates macrophage efferocytosis through downregulation of cell surface expression of CD36

Efferocytosis involves recognition, binding, ingestion and digestion of apoptotic cells by phagocytes. A variety of redundant receptors expressed on the surface of macrophages serve a key role in mediating the recognition and uptake of apoptotic cells (29). We found a time-dependent increase in the surface expression of a class B scavenger receptor CD36 in BMDMs in response to apoptotic PMN exposure, which coincided with decreased release of soluble CD36 without significant changes in its cytoplasmic fraction (Supplemental Fig. 1). The surface expression of CD36 was also found to increase in Rab11a-depleted BMDMs by siRNA compared to that in control siRNA-treated cells (Fig. 3A). Flow cytometry analysis revealed that overexpression of dominant negative Rab11a-S25N stimulated CD36 surface expression whereas macrophages expressing Rab11a-WT exhibited a decreased surface level of CD36 protein as compared to the vector control group (Fig. 3B). To investigate the role of CD36 in the enhanced apoptotic PMN uptake by Rab11a-depleted macrophages, the inhibitory effect by anti-CD36 blocking Ab was evaluated (Fig. 3C). An anti-CD36 blocking Ab (#ab23680; 20 μg/ml for 2 h) (30) not only abolished the augmented efferocytosis in Rab11a-depleted BMDMs but also significantly dampened efferocytosis in scrambled siRNA-treated macrophages (Fig. 3C). Taken together, these data identify CD36 as the major receptor responsible for the enhanced efferocytosis seen in Rab11a-depleted or -inactivated macrophages.

Rab11a facilitates surface expression of ADAM17 in macrophages

Ectodomain shedding of the extracellular portion of transmembrane proteins at or near the cell surface is a recognized mechanism for regulating surface expression and function of receptors (31). ADAM17 is a sheddase responsible for ectodomain shedding of a variety of cell surface proteins including CD36. The cleavage of surface receptors CD36 by ADAM17 leads to inhibition of efferocytosis (32). Since Rab11a is crucial in regulating intracellular and membrane trafficking (14-17), we tested the concept that Rab11a mediates the transport of ADAM17 from cytosol to cell surface. We thus studied whether surface expression of ADAM17 in BMDMs was modified in response to apoptotic PMN feeding. ADAM17 protein expression exhibited a time-dependent decrease on the cell surface and a concomitant increase in cytoplasmic fraction in response to apoptotic PMN feeding (Supplemental Fig. 2), suggesting that ADAM17 is unable to move to the cell membrane during efferocytosis. We next addressed whether ADAM17 localized in the Rab11 positive compartments. We observed a high degree of colocalization between Rab11a and ADAM17 in BMDMs by confocal immunofluorescence (Fig. 4A). Co-immunoprecipitation data confirmed this observation, and showed further that the association of Rab11a and ADAM17 was increased in response to apoptotic PMNs (Fig. 4B). Cell surface expression of ADAM17 was analyzed using flow cytometry to measure the amount of immunoreactive ADAM17 present in the plasma membrane. We found that cell surface ADAM17 expression was markedly reduced in Rab11a knockdown BMDMs compared to scrambled siRNA–treated cells (Fig. 4C). To ascertain whether Rab11a controlled intracellular ADAM17 trafficking, we examined the effects of Rab11a depletion by a specific siRNA on the cell surface and cytoplasmic expression of ADAM17 in BMDMs. As measured by immunoblotting, Rab11a knockdown decreased cell surface ADAM17 by approximately 65% but increased cytoplasmic ADAM17 2-fold (Fig. 4D and 4E), demonstrating the cytosolic accumulation of ADAM17 in the absence of Rab11a. Overall, these results indicate that Rab11a promotes ADAM17 trafficking to the cell surface from the cytosol.

To evaluate whether Rab11a inhibits surface expression of CD36 by modulation of ADAM17, macrophages were simultaneously transfected with ADAM17 siRNA with or without WT-Rab11a plasmid (Fig. 5A). Flow cytometry analysis showed that transfection with WT-Rab11a plasmid resulted in decreased surface CD36, whereas ADAM17 siRNA transfection completely rescued this effect and augmented surface expression of CD36 (Fig. 5B and 5C). Together, these observations show the important role of Rab11a in regulating the cell surface expression of CD36 through ADAM17 signaling.

Reduced expression of Rab11a in macrophages promotes clearance of apoptotic PMNs and accelerates resolution of inflammation

Clearance of apoptotic PMNs favors resolution of inflammation by down-regulating the inflammatory phenotype of activated macrophages (3,29). Based on our *in vitro* findings that Rab11a inactivation in macrophages was involved in phagocytosis of apoptotic PMNs (efferocytosis), we addressed whether Rab11a regulates resolution of lung inflammation through modulation of macrophage efferocytosis using an established *in vivo* model (19,26). By depleting alveolar macrophages in mice and then transplanting BMDMs that were genetically modified to have differential Rab11a expression, we specifically determined the

effect of Rab11a expression on the ability of macrophages to resolve LPS-induced lung inflammatory injury. As shown in Figure 6A, mice were first depleted of alveolar macrophages and then challenged with LPS, followed by intratracheal delivery of BMDMs transfected with a scrambled siRNA or specific Rab11a siRNA (Supplemental Fig. 3A). Following intratracheal instillation, the spatial distribution of macrophages in alveolar macrophage-depleted lungs receiving BMDMs treated with a scrambled siRNA or Rab11 siRNA is uniform and comparable (Supplemental Fig. 3B). As expected, LPS caused a significant increase in PMN counts in BAL fluid (Fig. 6B), lung MPO levels (Fig. 6C), protein level in BAL fluid (Fig. 6D), and edema formation (Fig. 6E) in control mice (without alveolar macrophage depletion) and alveolar macrophages-depleted mice at d 1, 3 and 5. Mice depleted of alveolar macrophages showed the delayed resolution of neutrophil infiltration (Fig. 6B and 6C), exuded protein (Fig. 6D), and lung edema (Fig. 6E) at d 7 and 10 following LPS challenge whereas these delayed responses were reversed by administration of control siRNA-treated BMDMs (Fig. 6B-E). Importantly, alveolar macrophage-depleted mice receiving Rab11 siRNA-transfected BMDMs showed further decreased PMN counts in BAL fluid (Fig. 6B), lung MPO (Fig. 6C), protein level in BAL fluid (Fig. 6D), and edema formation (Fig. 6E) compared with mice receiving scrambled siRNA-treated BMDMs at d 5, 7 and 10 following LPS challenge. HE staining indicated that lung tissues from control mice (without alveolar macrophage depletion) and alveolar macrophages-depleted mice were presented with severe histological changes, including alveolar congestion, exudates, and infiltration of inflammatory cells at d 5 following LPS challenge, in comparison with untreated mice (Fig. 6F). These histopathological alterations in lung tissues were dramatically ameliorated following administration of control siRNA-treated BMDMs and further improved by administration of Rab11a-treated BMDMs, as seen in the significantly reduced lung injury score (Fig. 6G). Consistently, at d 2 after injection of BMDMs (d 5 following LPS challenge), the number of macrophages containing apoptotic bodies or cells in BAL fluid was much higher in Rab11a-treated lungs than in control siRNA-treated lungs (Fig. 7A and 7B). To further demonstrate the role of Rab11a in the clearance of apoptotic PMNs *in vivo*, apoptotic mouse pHrodo™ Red (SE)-labeled PMNs were intratracheally injected into mice at d 2 following delivery of BMDMs and BAL fluid harvested 3 h later for determination of macrophage phagocytosis of PMNs. As shown in Figure 7C and 7D, the number of macrophages containing apoptotic PMNs in BAL was greater in mice receiving Rab11a siRNA-treated BMDMs than in those receiving control siRNA-treated BMDMs. To elucidate the potential mechanisms responsible for the accelerated resolution of lung inflammation by Rab11a depletion, we examined the levels of key inflammatory mediators in BAL fluid from mice receiving control and Rab11a siRNA-treated BMDMs. We found that the levels of proinflammatory cytokines TNF-α (Fig. 8A) and IL-6 (Fig. 8B) in the BAL fluid were elevated and reached peak levels at d 1 (TNF-α) or 3 (IL-6) following LPS challenge and then gradually decreased thereafter in control and alveolar macrophage-depleted mice. At d 5, 7 and 10 following LPS challenge, alveolar macrophage-depleted mice receiving scrambled siRNA-treated BMDMs showed lower levels of TNF-a (Fig. 8A) and IL-6 (Fig. 8B), which further decreased in alveolar macrophage-depleted mice receiving Rab11a-silenced BMDMs (Fig. 8A and 8B). In marked contrast, alveolar macrophage-depleted mice receiving Rab11a-silenced BMDMs had a remarkably increased level of anti-inflammatory cytokines TGF-β1 (Fig. 8C) and IL-10

(Fig. 8D) compared with those receiving scrambled siRNA-transfected BMDMs at d 5, 7 and 10 following LPS challenge. These data clearly indicate that macrophage Rab11a regulates resolution of LPS-induced lung inflammation and injury by modulating efferocytosis.

CD36 blockade abolishes enhanced resolution of lung inflammation following transplantation of Rab11a-depleted macrophages

We sought to examine the contribution of CD36-mediated efferocytosis in the enhanced resolution of lung inflammatory injury by Rab11a-depleted macrophages. CD36-blocking or isotype control Ab was intravenously injected at the same time as intratracheal instillation of BMDMs into the lung. CD36 blockade completely abrogated enhanced resolution of acute inflammatory lung injury by Rab11a depletion, as evidenced by increased PMN counts (Fig. 9A) and protein (Fig. 9B) in BAL fluid, edema formation (Fig. 9C) and lung injury score (Fig. 9D) compared to isotype control Ab. Thus, CD36-mediated phagocytosis of apoptotic cells may serve a key role in accelerating resolution of lung inflammatory injury by Rab11a depletion following LPS challenge.

Discussions

Here we identified a novel role of macrophage-expressed Rab11a GTPase in negatively regulating efferocytosis, thereby resolving acute lung inflammatory injury induced by sepsis. Our results showed that interaction of macrophages with apoptotic cells induced reduction of Rab11a activity in macrophages, which was central for up-regulating the surface expression of CD36 through blocking Rab11a-mediated ADAM17 trafficking to the macrophage cell membrane. We demonstrated that this pivotal step was important for the induction of phagocytosis of apoptotic PMNs. To elucidate the *in vivo* functional relevance of these observations, we showed that intratracheal instillation of macrophages, in which Rab11a was genetically depleted, enhanced the clearance of apoptotic PMNs and promoted resolution of lung inflammation and injury following LPS challenge. These findings clearly indicate that Rab11a acts as a negative regulator of phagocytosis of apoptotic PMNs and efferocytosis-dependent inflammation resolution. Therefore, targeting Rab11a activity in macrophages is a potential novel therapeutic strategy to reduce inflammation and injury associated with sepsis.

A crucial finding was that Rab11a activity itself in macrophages functioned as a brake on efferocytosis signaling; thus, Rab11 inactivation during efferocytosis is an important mechanism critical for promoting phagocytosis of apoptotic PMNs. This is evident by the findings that upon exposure of macrophages to apoptotic PMNs, Rab11a activity was rapidly reduced, and that depletion or inactivation of Rab11a in macrophages strongly increased phagocytosis of apoptotic PMNs. In a key experiment, we found that intratracheal instilling of macrophages in which Rab11a was silenced induced the uptake of apoptotic PMNs. In contrast to the role of reduced Rab11a in promoting macrophage efferocytosis, we found that Rab11a knockdown in macrophages inhibited phagocytosis of IgG-opsonized beads, consistent with previous findings (18). Macrophage efferocytosis is regulated by signaling mechanisms different from phagocytosis of cells opsonized with IgG (33-35). A study

showed that LPS and TNF-α inhibited the phagocytosis of apoptotic PMNs by human macrophages while having no effect on the phagocytosis of IgG-opsonized erythrocytes (33). Moreover, the efferocytic engulfment of apoptotic cells by macrophages suppressed pro-inflammatory signaling and activated pro-resolving signaling, whereas macrophage engulfment of IgG-opsonized pathogens by FcγR activated the release of proinflammatory cytokines (36,37). Although the phagocytosis of bacteria and apoptotic cells relies on the same cellular machinery, the signaling mechanisms are quite different (38). Our results combined with other findings (18) suggest a specialized role of Rab11a in mediating phagocytosis of apoptotic PMNs as opposed to pathogens bound to IgG.

The scavenger receptor CD36, a transmembrane glycoprotein member of the class B scavenger receptor family, is expressed on the surface of multiple cell types, including macrophages (39). CD36 is important for apoptotic cell recognition and uptake (40) and serves as a critical regulator of phagocytosis in sepsis (41). We observed that Rab11a activation down-regulated CD36 surface expression, which in turn decreased efferocytosis and delayed resolution of lung inflammation and injury. Confocal imaging and flow cytometry data showed higher surface expression of CD36 in Rab11a-depleted or Rab11a-inactivated macrophages as compared to controls. Importantly, CD36 blockade abrogated the enhanced efferocytosis response and accelerated resolution of lung inflammation and injury seen following Rab11a depletion. Thus, relative CD36 expression on the macrophage cell surface has a requisite role in the mechanism of Rab11a-mediated phagocytosis of apoptotic cells.

An important question is how Rab11a regulates CD36 surface expression in macrophages. CD36 localizes in Rab11 containing-vesicle (42), suggesting that Rab11 may facilitate the trafficking of CD36 to the cell membrane through recycling endosomes. However, this does not appear to be the case in the present study because depletion of Rab11a increased CD36 surface expression in macrophages. Surface expression of CD36 is highly regulated by its cleavage and shedding (32). The transmembrane protease ADAM17 proteolytically cleaves efferocytosis receptors including CD36, tyrosine kinase Mer (MerTK), and lectin-like oxidized LDL receptor 1 (LOX-1) on the cell surface (43,44). ADAM17 membrane proximal cleavage of its substrates releases almost the entire extracellular domain of CD36 (32). Our study supports the novel role of Rab11a in mediating ADAM17 transport to the macrophage plasma membrane, thereby regulating phagocytosis of apoptotic PMN through cleavage of CD36 and reducing CD36 cell surface expression. We showed that in response to apoptotic cell feeding, Rab11a activity was rapidly reduced while ADAM17 expression on the cell surface decreased in association with increased cytoplasmic ADAM17 fraction. Further, Rab11a was highly colocalized with ADAM17 in macrophages under basal conditions. Although the association between Rab11a and ADAM17 increased in response to apoptotic PMNs exposure, ADAM17 trafficking to the cell membrane decreased due to the inhibition of Rab11a activity. In Rab11-depleted macrophages, ADAM17 accumulated in the cytosol and was unable to reach the cell surface. These results demonstrate the crucial role of Rab11a activity in mediating ADAM17 trafficking in macrophages. Finally, ADAM17 knockdown completely reversed the decreased surface expression of CD36 caused by overexpression of WT-Rab11a protein. In toto, our results show the requisite role of

Rab11a in down-regulating the surface expression of CD36 in macrophages through facilitating the trafficking of ADAM17 to the macrophage plasma membrane.

To address the *in vivo* relevance of our findings, we used an established murine model of LPS-induced lung inflammation and injury (19). We demonstrated that Rab11a in macrophages functioned as a negative regulator of efferocytosis-dependent resolution of lung inflammation and injury. Efferocytosis is a central mechanism for restoration of tissue homeostasis and is critical for recovery from inflammation and injury (45). We observed that airway instillation of Rab11a-silenced macrophages enhanced anti-inflammatory response and accelerated resolution of lung inflammation and injury. This pro-resolution response was associated with increased number of macrophages containing either apoptotic bodies or PMNs in BAL fluid. Also, inhibition of efferocytosis by anti-CD36 blocking Ab reversed the protective effect of instilled Rab11a-depleted macrophages. Although our results support the role of CD36 downregulation in reducing clearance of apoptotic PMNs and enhancing inflammation in response to LPS (39), they describe for the first time the underlying Rab11a- and ADAM17-regulated mechanism of fine-tuning of the cell surface expression of CD36 and efferocytosis-mediated resolution of inflammation.

In summary, the present studies demonstrate the essential role of Rab11a activation in macrophages as a “choke point” for regulating phagocytosis of PMN and thereby resolving inflammatory lung injury induced by endotoxin. Apoptotic PMN feeding induced Rab11a inactivation in macrophages, which in turn increased surface levels of CD36 through blocking ADAM17 trafficking to the cell membrane and subsequent ADAM17-mediated cleavage of CD36. Increased CD36 surface expression in macrophages as result of Rab11a inactivation thus promotes effective clearance of apoptotic PMNs and resolution of inflammation and tissue injury (Fig. 10). Our findings provide new insights into mechanisms of efferocytosis regulated by Rab11a, showing that enhanced macrophage efferocytosis due to Rab11a inactivation accelerates resolution of lung inflammation. The results point to a potential therapeutic approach whereby modulating Rab11a activity in macrophages enhances phagocytosis of dying PMNs and resolve acute lung injury.

Supplementary Material

Refer to Web version on PubMed Central for supplementary material.

Acknowledgments

We thank Maricela Castellon (Department of Anesthesiology, University of Illinois College of Medicine) for technical assistance.

This work was supported by NIH NHLBI grants HL104092 (GH) and Natural Science Foundation of China 81470259 (GH).

References

1. Rock KL, Lai JJ, Kono H. Innate and adaptive immune responses to cell death. Immunol Rev. 2011; 243:191–205. [PubMed: 21884177]
2. Ortega-Gomez A, Perretti M, Soehnlein O. Resolution of inflammation: an integrated view. EMBO Mol Med. 2013; 5:661–674. [PubMed: 23592557]

3. Korns D, Frasch SC, Fernandez-Boyanapalli R, Henson PM, Bratton DL. Modulation of macrophage efferocytosis in inflammation. Front Immunol. 2011; 2:57. [PubMed: 22566847]
4. Voll RE, Herrmann M, Roth EA, Stach C, Kalden JR. Immunosuppressive effect of apoptotic cells. Nature. 1997; 390:350–351. [PubMed: 9389474]
5. Fadok VA, Bratton DL, Rose DM, Pearson A, Ezekewitz RA, Henson PM. A receptor for phosphatidyiserine-specific clearance of apoptotic cells. Nature. 2000; 405:85–90. [PubMed: 10811223]
6. Basil MC, Levy BD. Specialized pro-resolving mediators: endogenous regulators of infection and inflammation. Nat Rev Immunol. 2016; 16:51–67. [PubMed: 26688348]
7. Headland SE, Norling LV. The resolution of inflammation: Principles and challenges. Semin Immunol. 2015; 27:149–160. [PubMed: 25911383]
8. Ravichandran KS, Lorenz U. Engulfment of apoptotic cells: signals for a good meal. Nat Rev Immunol. 2007; 7:964–974. [PubMed: 18037898]
9. Serhan CN, Savill J. Resolution of inflammation: the beginning programs the end. Nat Immunol. 2005; 6:1191–1197. [PubMed: 16369558]
10. Poon IK, Lucas CD, Rossi AG, Ravichandran KS. Apoptotic cell clearance: basic biology and therapeutic potential. Nat Rev Immunol. 2014; 14:166–180. [PubMed: 24481336]
11. Hochreiter-Hufford A, Ravichandran KS. Clearing the dead: apoptotic cell sensing, recognition, engulfment, and digestion. Cold Spring Harb Perspect Biol. 2013; 5:a008748. [PubMed: 23284042]
12. Schwartz SL, Cao C, Pylypenko O, Rak A, Wandinger-Ness A. Rab GTPases at a glance. J Cell Sci. 2007; 120:3905–3910. [PubMed: 17989088]
13. Stenmark H. Rab GTPases as coordinators of vesicle traffic. Nat Rev Mol Cell Biol. 2009; 10:513–525. [PubMed: 19603039]
14. Bhuin T, Roy JK. Rab11 in disease progression. Int J Mol Cell Med. 2015; 4:1–8. [PubMed: 25815277]
15. Welz T, Wellbourne-Wood J, Kerkhoff E. Orchestration of cell surface proteins by Rab11. Trends Cell Biol. 2014; 24:407–415. [PubMed: 24675420]
16. Grant BD, Donaldson JG. Pathways and mechanisms of endocytic recycling. Nat Rev Mol Cell Biol. 2009; 10:597–608. [PubMed: 19696797]
17. Yan Z, Wang ZG, Segev N, Hu S, Minshall RD, Dull RO, Zhang M, Malik AB, Hu G. Rab11a Mediates Vascular Endothelial-Cadherin Recycling and Controls Endothelial Barrier Function. Arterioscler Thromb Vasc Biol. 2016; 36:339–349. [PubMed: 26663395]
18. Cox D, Lee DJ, Dale BM, Calafat J, Greenberg S. A Rab11-containing rapidly recycling compartment in macrophages that promotes phagocytosis. Proc Natl Acad Sci USA. 2000; 97:680–685. [PubMed: 10639139]
19. Yang Z, Sun D, Yan Z, Reynolds AB, Christman JW, Minshall RD, Malik AB, Zhang Y, Hu G. Differential role for p120-catenin in regulation of TLR4 signaling in macrophages. J Immunol. 2014; 193:1931–1941. [PubMed: 25015829]
20. Hu G, Ye RD, Dinauer MC, Malik AB, Minshall RD. Neutrophil caveolin-1 expression contributes to mechanism of lung inflammation and injury. Am J Physiol Lung Cell Mol Physiol. 2008; 294:L178–L186. [PubMed: 17993589]
21. Kang J, Park KH, Kim JJ, Jo EK, Han MK, Kim UH. The role of CD38 in Fcγ receptor (FcγR)-mediated phagocytosis in murine macrophages. J Biol Chem. 2012; 287:14502–14514. [PubMed: 22396532]
22. Moon C, Lee YJ, Park HJ, Chong YH, Kang JL. N-acetylcysteine inhibits RhoA and promotes apoptotic cell clearance during intense lung inflammation. Am J Respir Crit Care Med. 2010; 181:374–387. [PubMed: 19965809]
23. Miksa M, Komura H, Wu R, Shah KG, Wang P. A novel method to determine the engulfment of apoptotic cells by macrophages using pHrodo succinimidyl ester. J Immunol Methods. 2009; 342:71–77. [PubMed: 19135446]
24. Esmann L, Idel C, Sarkar A, Hellberg L, Behnen M, Möller S, van Zandbergen G, Klinger M, Köhl J, Bussmeyer U, Solbach W, Laskay T. Phagocytosis of apoptotic cells by neutrophil granulocytes:

diminished proinflammatory neutrophil functions in the presence of apoptotic cells. J Immunol. 2010; 184:391–400. [PubMed: 19949068]

25. Wu J, Yan Z, Schwartz DE, Yu J, Malik AB, Hu G. Activation of NLRP3 inflammasome in alveolar macrophages contributes to mechanical stretch-induced lung inflammation and injury. J Immunol. 2013; 190:3590–3599. [PubMed: 23436933]
26. Suzuki T, Arumugam P, Sakagami T, Lachmann N, Chalk C, Sallese A, Abe S, Trapnell C, Carey B, Moritz T, Malik P, Lutzko C, Wood RE, Trapnell BC. Pulmonary macrophage transplantation therapy. Nature. 2014; 514:450–454. [PubMed: 25274301]
27. Wang YL, Malik AB, Sun Y, Hu S, Reynolds AB, Minshall RD, Hu G. Innate immune function of the adherens junction protein p120-catenin in endothelial response to endotoxin. J Immunol. 2011; 186:3180–3187. [PubMed: 21278343]
28. D'Alessio FR, Tsushima K, Aggarwal NR, Mock JR, Eto Y, Garibaldi BT, Files DC, Avalos CR, Rodriguez JV, Waickman AT, Reddy SP, Pearse DB, Sidhaye VK, Hassoun PM, Crow MT, King LS. Resolution of experimental lung injury by monocyte-derived inducible nitric oxide synthase. J Immunol. 2012; 189:2234–2245. [PubMed: 22844117]
29. McCubbrey AL, Curtis JL. Efferocytosis and lung disease. Chest. 2013; 143:1750–1757. [PubMed: 23732585]
30. Valente AJ, Yoshida T, Clark RA, Delafontaine P, Siebenlist U, Chandrasekar B. Advanced oxidation protein products induce cardiomyocyte death via Nox2/Rac1/superoxide-dependent TRAF3IP2/JNK signaling. Free Radic Biol Med. 2013; 60:125–135. [PubMed: 23453926]
31. Liu C, Xu P, Lamouille S, Xu J, Derynck R. TACE-mediated ectodomain shedding of the type I TGF-beta receptor downregulates TGF-beta signaling. Mol Cell. 2009; 35:26–36. [PubMed: 19595713]
32. Driscoll WS, Vaisar T, Tang J, Wilson CL, Raines EW. Macrophage ADAM17 deficiency augments CD36-dependent apoptotic cell uptake and the linked anti-inflammatory phenotype. Circ Res. 2013; 113:52–61. [PubMed: 23584255]
33. Michlewska S, Dransfield I, Megson IL, Rossi AG. Macrophage phagocytosis of apoptotic neutrophils is critically regulated by the opposing actions of pro-inflammatory and anti-inflammatory agents: key role for TNF-α. FASEB J. 2009; 23:844–854. [PubMed: 18971259]
34. Rossi AG, McCutcheon JC, Roy N, Chilvers ER, Haslett C, Dransfield I. Regulation of macrophage phagocytosis of apoptotic cells by cAMP. J Immunol. 1998; 160:3562–3568. [PubMed: 9531319]
35. Michlewska S, McColl A, Rossi AG, Megson IL, Dransfield I. Clearance of dying cells and autoimmunity. Autoimmunity. 2007; 40:267–273. [PubMed: 17516208]
36. Yamamoto K, Johnston RB Jr. Dissociation of phagocytosis from stimulation of the oxidative metabolic burst in macrophages. J Exp Med. 1984; 159:405–416. [PubMed: 6319532]
37. Fadok VA, Bratton DL, Konowal A, Freed PW, Westcott JY, Henson PM. Macrophages that have ingested apoptotic cells in vitro inhibit proinflammatory cytokine production through autocrine/paracrine mechanisms involving TGF-beta, PGE2, and PAF. J Clin Invest. 1998; 101:890–898. [PubMed: 9466984]
38. Gruenberg J, Maxfield FR. Membrane transport in the endocytic pathway. Curr Opin Cell Biol. 1995; 7:552–563. [PubMed: 7495576]
39. Zamora C, Canto E, Nieto JC, Angels Ortiz M, Juarez C, Vidal S. Functional consequences of CD36 downregulation by TLR signals. Cytokine. 2012; 60:257–265. [PubMed: 22795952]
40. Greenberg ME, Sun M, Zhang R, Febbraio M, Silverstein R, Hazen SL. Oxidized phosphatidylserine-CD36 interactions play an essential role in macrophage-dependent phagocytosis of apoptotic cells. J Exp Med. 2006; 203:2613–2625. [PubMed: 17101731]
41. Leelahavanichkul A, Bocharov AV, Kurlander R, Baranova IN, Vishnyakova TG, Souza AC, Hu X, Doi K, Vaisman B, Amar M, Sviridov D, Chen Z, Remaley AT, Csako G, Patterson AP, Yuen PS, Star RA, Eggerman TL. Class B scavenger receptor types I and II and CD36 targeting improves sepsis survival and acute outcomes in mice. J Immunol. 2012; 188:2749–2758. [PubMed: 22327076]

42. Kessler A, Tomas E, Immler D, Meyer HE, Zorzano A, Eckel J. Rab11 is associated with GLUT4-containing vesicles and redistributes in response to insulin. Diabetologia. 2000; 43:1518–1527. [PubMed: 11151761]

43. Thorp E, Vaisar T, Subramanian M, Mautner L, Blobel C, Tabas I. Shedding of the Mer tyrosine kinase receptor is mediated by ADAM17 protein through a pathway involving reactive oxygen species, protein kinase Cdelta, and p38 mitogen-activated protein kinase (MAPK). J Biol Chem. 2011; 286:33335–33344. [PubMed: 21828049]

44. Zhao XQ, Zhang MW, Wang F, Zhao YX, Li JJ, Wang XP, Bu PL, Yang JM, Liu XL, Zhang MX, Gao F, Zhang C, Zhang Y. CRP enhances soluble LOX-1 release from macrophages by activating TNF-alpha converting enzyme. J Lipid Res. 2011; 52:923–933. [PubMed: 21364202]

45. Patel BV, Wilson MR, Takata M. Resolution of acute lung injury and inflammation: a translational mouse model. Eur Respir J. 2012; 39:1162–1170. [PubMed: 22005920]

Abbreviations used in this article

ADAM 17	a disintegrin and metalloproteinase 17
BAL	Bronchoalveolar lavage
BMDM	bone marrow–derived macrophage
MPO	myeloperoxidase
pHrodo-SE	pHrodo succinimidyl ester
PMNs	polymorphonuclear neutrophils
PS	phosphatidylserine
Rab	Ras-related proteins in brain
RIPA	radioimmunoprecipitation assay
siRNA	small interfering RNA

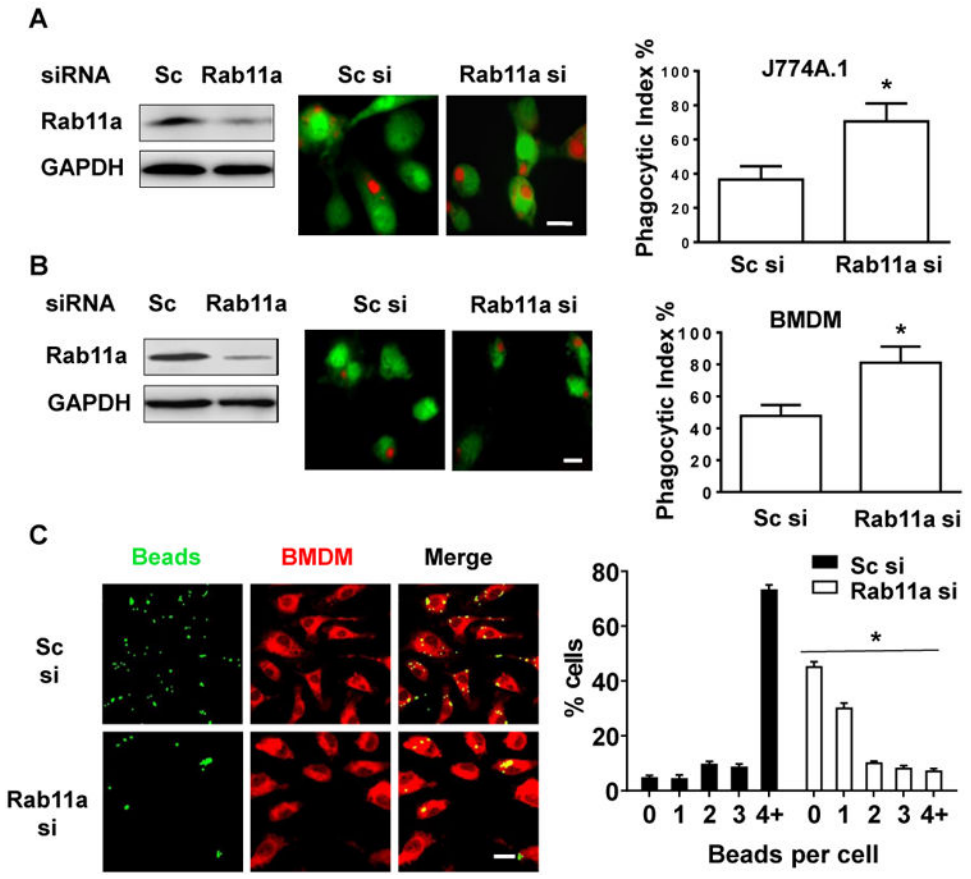

Figure 1. Depletion of Rab11a enhances macrophage phagocytosis of apoptotic PMNs

J774A.1 macrophages (A) and BMDMs (B, C) were transfected with scrambled (Sc) or Rab11a siRNA (si). At 48 h post siRNA transfection, the transfected macrophages were labelled with CellTracker™ Green and incubated with CellTracker™ Red-labelled apoptotic PMNs (A, B) at 1:10 ratio for 2 h. The cells were then mounted on a slide and analyzed by fluorescent microscopy. Scale bars, 10 μm. (**A**) Rab11a knockdown increased the phagocytosis of apoptotic PMNs in J774A.1 macrophages. *Left*, Rab11a protein expression in macrophages at 48 h post siRNA transfection; *Middle*, representative fluorescent images showing macrophages engulfing apoptotic PMNs; *Right*, phagocytic index based on the fluorescent images. (**B**) Rab11a knockdown increased the phagocytosis of apoptotic PMNs in BMDMs. *Left*, Rab11a protein expression in BMDMs at 48 h post siRNA transfection; *Middle*, representative fluorescent images macrophages engulfing an apoptotic PMNs; *Right*, phagocytic index based on the fluorescent images. (**C**) Rab11a knockdown decreased the phagocytosis of IgG-opsonized fluorescent latex beads in BMDMs. The transfected BMDMs were labelled with CellTracker™ Red and incubated with FITC-labelled, IgG-opsonized latex beads (green) for 20 min. The cells were then mounted on a slide and analyzed by fluorescent microscopy. *Left*, representative fluorescent images showing macrophages engulfing IgG-opsonized latex beads; *Right*, phagocytic index based on the fluorescent images. Scale bars, 10 μm. Data were obtained from three independent cultures, each performed in triplicate. Each bar represents the mean ± SEM (n=3). Statistical

significance was calculated by Student's *t*-test (A, B) or two-way ANOVA followed by Student's *t*-test (**C**). *P<0.05 vs. Sc siRNA groups.

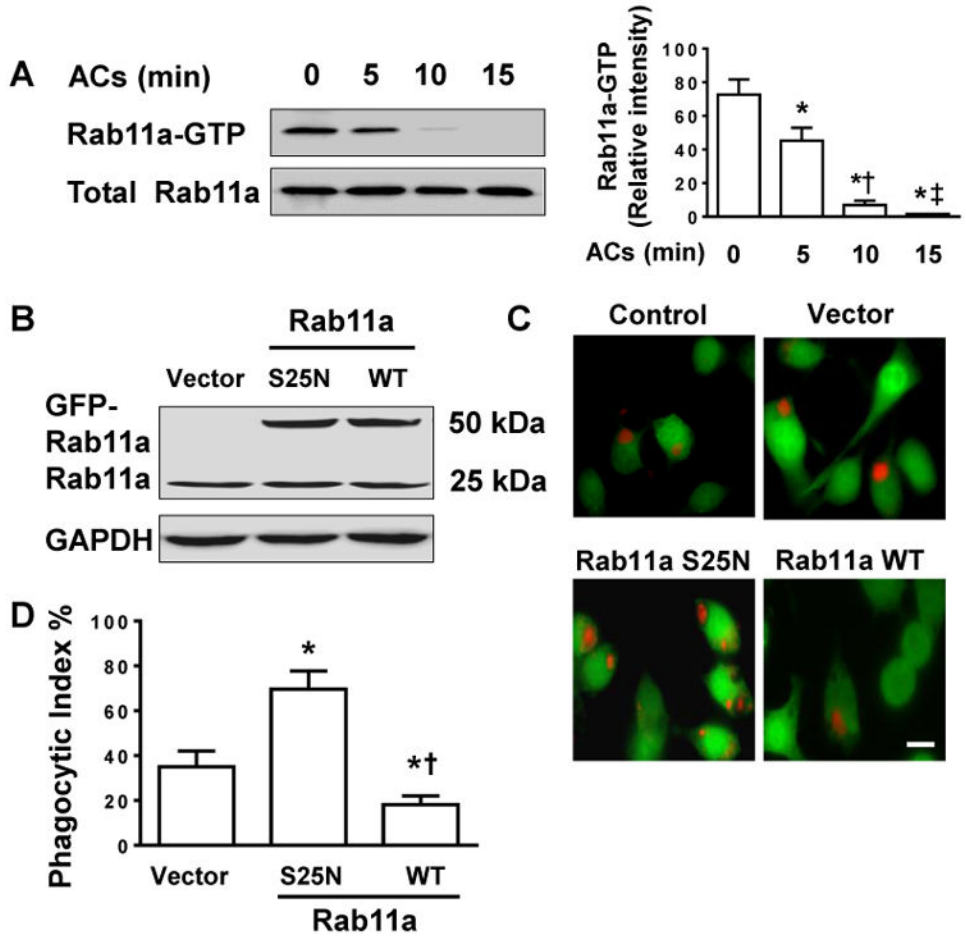

Figure 2. Rab11a Inactivation promotes clearance of apoptotic PMNs

(**A**) Time-dependent Rab11a inactivation in BMDMs in response to apoptotic PMNs (ACs) feeding. BMDMs were co-cultured with apoptotic PMNs at 1:10 ratio for ~15 min. Lysates from macrophages were analyzed by Rab11a Activation Assay Kit. *Left*, pull-down experiment showing the content of Rab11-GTP in BMDMs stimulated with ACs; *Right*, quantification of three independent experiments is provided. (**B**) Endogenous and exogenous expression of Rab11a protein in BMDMs analyzed by Western blots. BMDMs were transfected with vector, dominant negative (S25N), or wild type (WT) Rab11a cDNA. (**C**) Representative fluorescent imaging of phagocytosis of ACs. The transfected BMDMs were labeled with CellTracker™ Green. After incubation of macrophages with CellTracker™ Red-labelled apoptotic PMNs for 2 h, macrophage efferocytosis was visualized using fluorescence microscopy. Scale bar, 10 μm. (**D**) Phagocytic index. Data were obtained from three independent cultures, each performed in triplicate, and expressed as mean ± SEM. The P value was calculated by one-way ANOVA followed by Student's *t*-test. *P<0.05 vs. control (A) or vector group (D); †P <0.05 vs. 5 min group (A) or S25N group (D); ‡ P <0.05 vs. 10 min group (A).

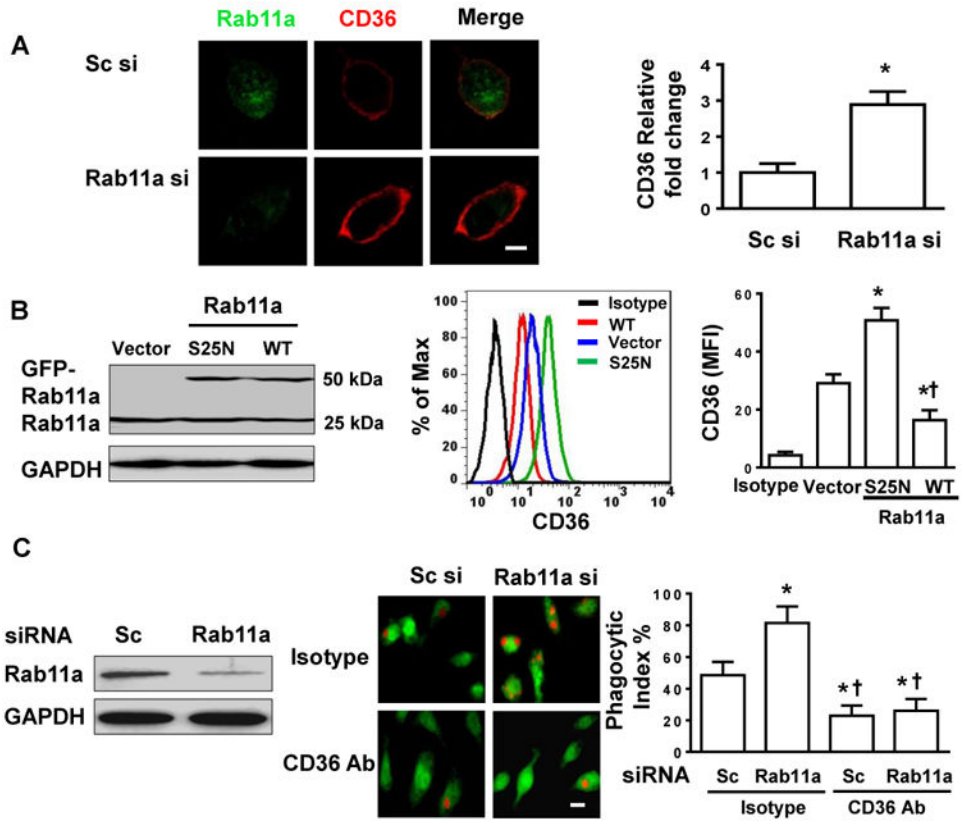

Figure 3. Rab11a regulates macrophage cell surface expression of CD36

(**A**) Rab11a knockdown increased surface expression of CD36. BMDMs were transfected with a scrambled (Sc) or Rab11a siRNA. At 48 h post transfection, cells were stained with an anti-Rab11a Ab (green) and an anti-CD36 Ab (red) targeting an extracellular epitope, and cells were left intact (not permeabilized). *Left*, representative confocal images showing surface expression of CD36 by confocal microscopy*; Right*, quantitative fluorescence intensity of membrane CD36 expression. n=4. *P<0.05 vs Sc si control group. Scale bar, 10 μm. (**B**). Effects of Rab11a activation on surface expression. BMDMs were transfected with vector, dominant negative (S25N), or wild type (WT) Rab11a cDNA. At 48 h post transfection, cells were stained with an anti-CD36 Ab. *Left*, endogenous and exogenous expression of Rab11a protein in BMDMs analyzed by Western blots; *Middle*, surface expression of CD36 was assessed by flow cytometry; *Right*, quantitative data showing changes in mean fluorescent intensity (MFI) of CD36. n=4. * P<0.05 vs. vector group. † P<0.05 vs. S25N group. (**C**) CD36 blockade abolished Rab11a-depletion-mediated increase in phagocytosis of apoptotic PMNs. At 48 h after transfection of BMDMs with Sc siRNA or Rab11a siRNA, cells were treated with CD36 blocking Ab (20 μg/ml) or isotype Ab for 2 h. Macrophages were then labelled with CellTracker™ Green and co-incubated with CellTracker™ Red labelled apoptotic PMNs for 2 h. Phagocytosis of apoptotic PMNs was visualized using fluorescence microscopy. *Left*, Rab11a protein expression in macrophages at 48 h post siRNA transfection; *Middle*, representative fluorescent images showing macrophages engulfing apoptotic PMNs; *Right*, phagocytic index based on the fluorescent images. Scale bar, 10 μm. n=4. Statistical significance was calculated by Student's *t*-test (A)

or one-way ANOVA followed by Student's *t*-test (B, C). * P<0.05 vs. Sc siRNA+Isotype groups, † P<0.05 vs. corresponding Isotype group.

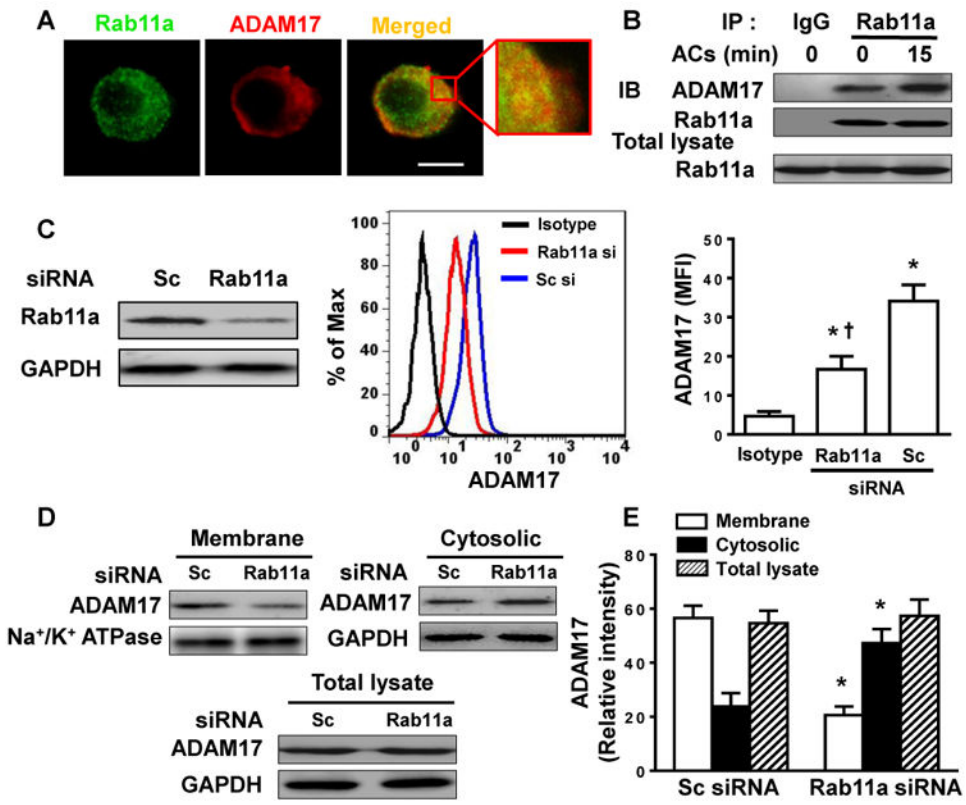

Figure 4. Rab11a regulates macrophage cell surface ADAM17 expression

(**A**). Rab11a colocalized with ADAM17 in BMDMs. BMDMs were immunostained with anti-Rab11a (green) and anti-ADAM17 (red) Abs. Representative confocal images show colocalization (yellow) of Rab11a and ADAM17. Scale bar, 10 μm. (**B**) Rab11a associated with ADAM17 in BMDMs. BMDMs were incubated with apoptotic PMNs (ACs) for 15 min, immunoprecipitated (IP) with Rab11a, and immunoblotted (IB) with an anti–ADAM17 Ab. (**C**). Effects of Rab11a knockdown on cell surface expression of ADAM17. BMDMs were transfected with a scrambled (Sc) siRNA or Rab11a siRNA. *Left*, Rab11a protein expression in macrophages at 48 h post siRNA transfection; *Middle*, surface expression of ADAM17 was analyzed by flow cytometry; *Right*, quantitative data showing changes in mean fluorescent intensity (MFI) of ADAM17. n=4. Statistical significance was calculated by one-way ANOVA followed by Student's *t*-test. *P<0.05 vs. Isotype groups, †P<0.05 vs. Sc siRNA group. (**D**). Effects of Rab11a depletion on subcellular localization of ADAM17 in BMDMs. *Top (left)*, immunoblot showing the levels of ADAM17 expression on cell surface; *Top (right)*, immunoblot showing the levels of ADAM17 expression in cytosolic fraction; *Bottom*, immunoblot showing the total levels of ADAM17 expression. (**E**) Protein quantification by densitometry. Bar graph shows the relative abundance of ADAM17 protein (normalized to that of loading controls) from 3 independent experiments. Statistical significance was calculated by Student's *t*-test. *P<0.05 vs. corresponding Sc siRNA groups.

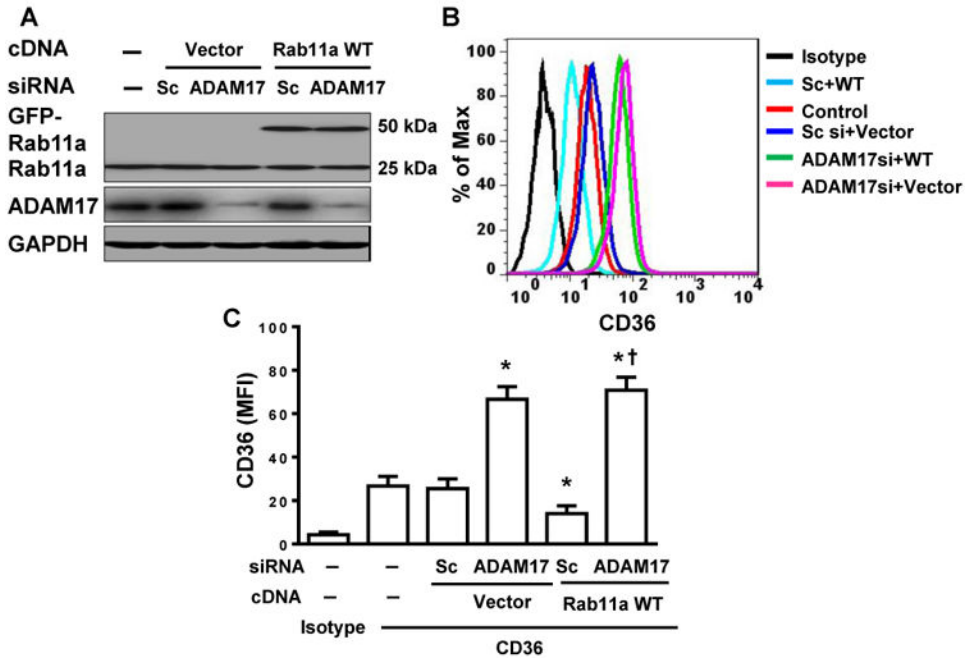

Figure 5. Rab11a deletion increase surface levels of CD36 through inhibiting ADAM17 trafficking

BMDMs were transfected with scrambled (Sc) or ADAM17 siRNA and plasmids encoding vector or GFP-tagged wild type (WT) Rab11a. (**A**) Protein expression of endogenous Rab11a and ADAM17 and exogenous expression of Rab11a protein in BMDMs were analyzed by Western blots. (**B**) Surface expression of CD36 was assessed by flow cytometry. (**C**) Quantitative data showing changes in mean fluorescent intensity (MFI) of CD36. n=4. Statistical significance was calculated by one-way ANOVA followed by Student's *t*-test. * P<0.05 vs. control groups (Vector + Sc). † P<0.05 vs. corresponding Sc group (Rab11a WT).

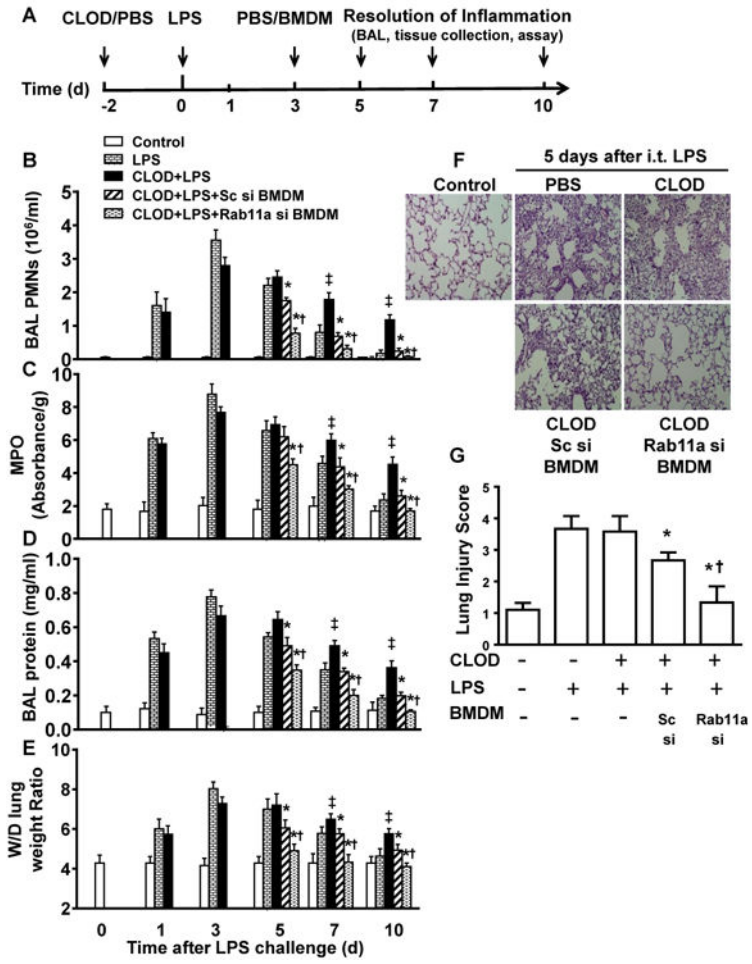

Figure 6. Role of macrophage Rab11a in resolution of lung inflammation and injury

(**A**) Experimental protocols of induction and time course of resolution of lung inflammation post-LPS challenge in wild type mice. Following depletion of alveolar macrophages with clodronate liposome (CLOD), mice were intratracheally instilled with LPS. BMDMs isolated from donor mice were cultured and transfected with a scramble siRNA (Sc) or Rab11a siRNA. After 48 h, the efficiency of transfection was evaluated by Western blot analysis. BMDMs treated with a Sc siRNA or Rab11a siRNA were i.t. injected into alveolar macrophages-depleted mice. Resolution of lung inflammatory injury was evaluated at d 1, 3, 5, 7 and 10 post LPS challenge as described in *Materials and Methods*. n = 6 animals/group/time point. (**B**) Neutrophil (PMN) counts in the BAL fluid. (**C**) PMN sequestration in lungs as assessed by MPO activity. (**D**) Pulmonary vascular protein permeability as determined by protein concentration of BAL fluid. (**E**) Pulmonary edema formation measured by wet-to-dry (W/D) lung weight ratio. (**F**) Histological analysis of lung tissue by hematoxylin and eosin staining (40× magnification). (**G**) Histopathological mean lung injury scores from low-power (20×) sections. Measurements were performed in triplicate for data analysis. Statistical significance was calculated by two- (B-E) or one-way (G) ANOVA followed by Tukey's multiple comparison tests. *P<0.05 vs. corresponding CLOD+LPS groups; †P<0.05 vs. corresponding Sc siRNA groups; ‡ P<0.05 vs. corresponding LPS groups.

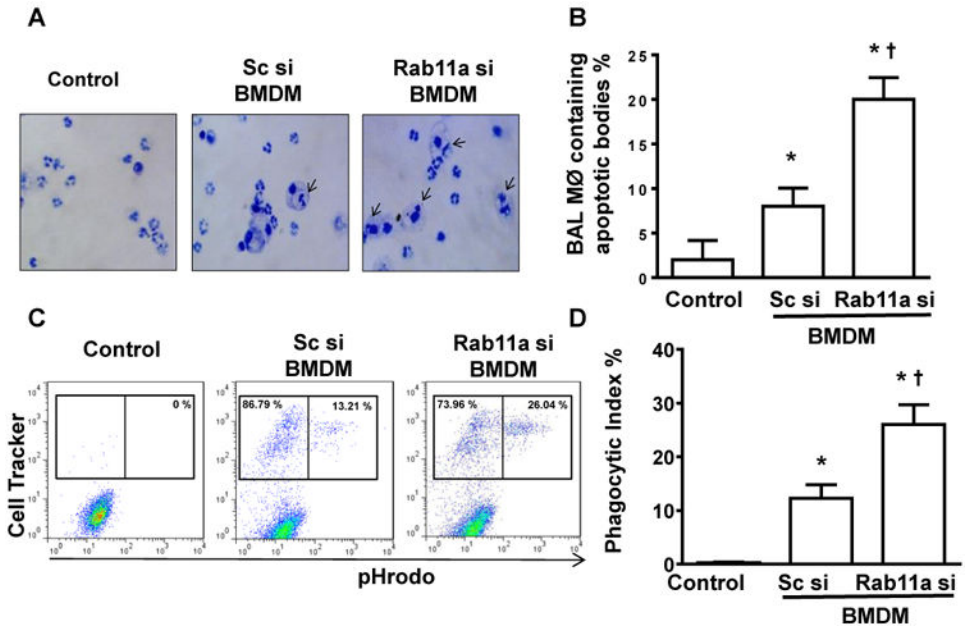

Figure 7. Rab11 depletion increases phagocytosis of apoptotic bodies or PMNs by alveolar macrophages

Experimental protocols of induction and time course of resolution of lung inflammation post-LPS challenge are shown as Fig. 6A. Alveolar macrophage-depleted mice were intratracheally administered with vehicle (PBS, Control), or BMDMs transfected with scrambled (Sc) or Rab11a siRNA. (**A**) Representative photomicrographs of cytospin preparations of BAL cells 2 d after injection of BMDMs. Arrows indicate apoptotic bodies. Original magnification 40×. (**B**) Quantification of BAL fluid macrophages (MΦ) containing apoptotic bodies. n = 6 / each group. *P < 0.05 vs. control group; †P < 0.05 vs. Sc si group. (**C**) Effects of Rab11a depletion on phagocytosis of apoptotic PMNs *in vivo* following LPS challenge. 1.0×10^7 pHrodo™ Red (SE)-labeled apoptotic PMNs was intratracheally instilled 2 d following CellTracker™ Green-labeled BMDM transplantation (2.0×10^6). At 3 h after instillation of apoptotic PMNs, BAL was performed, washed, and analyzed by flow cytometry (pH to 10 with 0.003 M sodium carbonate). Representative flow cytometric dot plots demonstrating changes in the proportion of macrophages engulfing pHrodo-stained apoptotic PMNs are shown. (**D**) Phagocytic index was calculated by average percent of macrophage containing apoptotic PMNs. n = 6 / each group. Measurements were performed in triplicate for data analysis. Statistical significance was calculated by one-way ANOVA followed by Student's *t*-test. *P < 0.05 vs. control group; †P<0.05 vs. Sc si group.

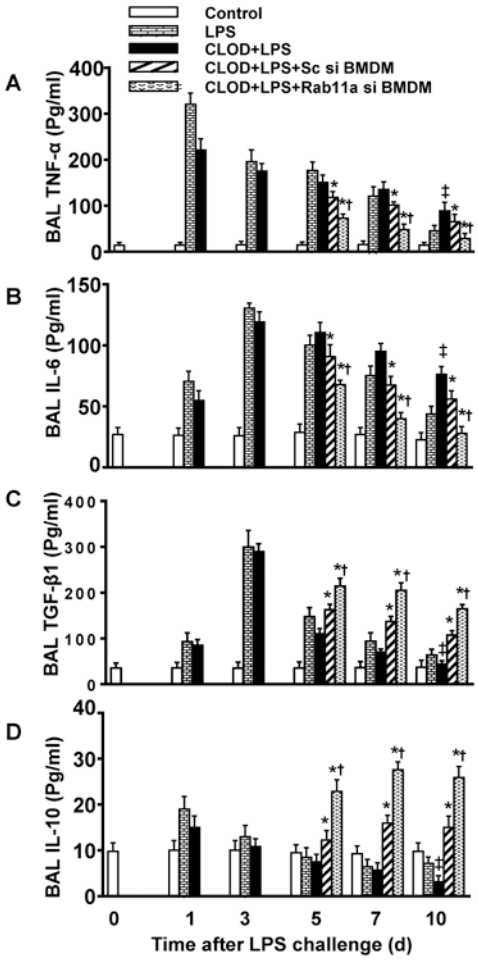

Figure 8. Macrophage Rab11a regulates the release of cytokines

Experimental protocols of induction and time course of resolution of lung inflammation post-LPS challenge are shown as Fig. 6A. (**A-D**) Levels of TNF-α (A) and IL-6 (B), TGF-β1 (C), and IL-10 (D) in BAL fluid measured by ELISA. n = 6 /each group. Measurements were performed in triplicate for data analysis. Statistical significance was calculated by two-way ANOVA followed by Tukey's multiple comparison tests. *P < 0.05 vs. corresponding CLOD+LPS groups; †P < 0.05 vs. corresponding Sc siRNA groups; ‡ P<0.05 vs. corresponding LPS groups. CLOD, clodronate liposome.

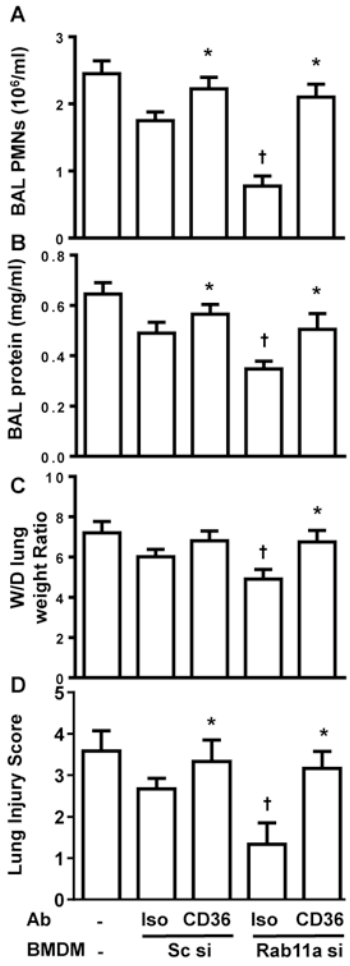

Figure 9. CD36 blockade abolishes Rab11a depletion-induced resolution of lung inflammation

Experimental protocols of induction and time course of resolution of lung inflammation post-LPS challenge are shown as Fig. 6A. CD36-blocking or isotype control (Iso) Ab was intravenously injected while BMDMs were i.t. admonished into the lung. At d 2 after injection of BMDMs, BAL and lung tissue was collected and tested. (**A**) PMNs in BAL fluid were enumerated to evaluate lung airspace inflammation. (**B**) Pulmonary vascular protein permeability as determined by protein concentration of BAL fluid. (**C**) Pulmonary edema formation measured by wet-to-dry (W/D) lung weight ratio. (**D**) Histopathological mean lung injury scores from low-power (20×) sections. n = 6 animals /group. Measurements were performed in triplicate for data analysis. Statistical significance was calculated by one-way ANOVA followed by Student's *t*-test. *P<0.05 vs. corresponding Iso group. †P<0.05 vs. Sc +Iso group.

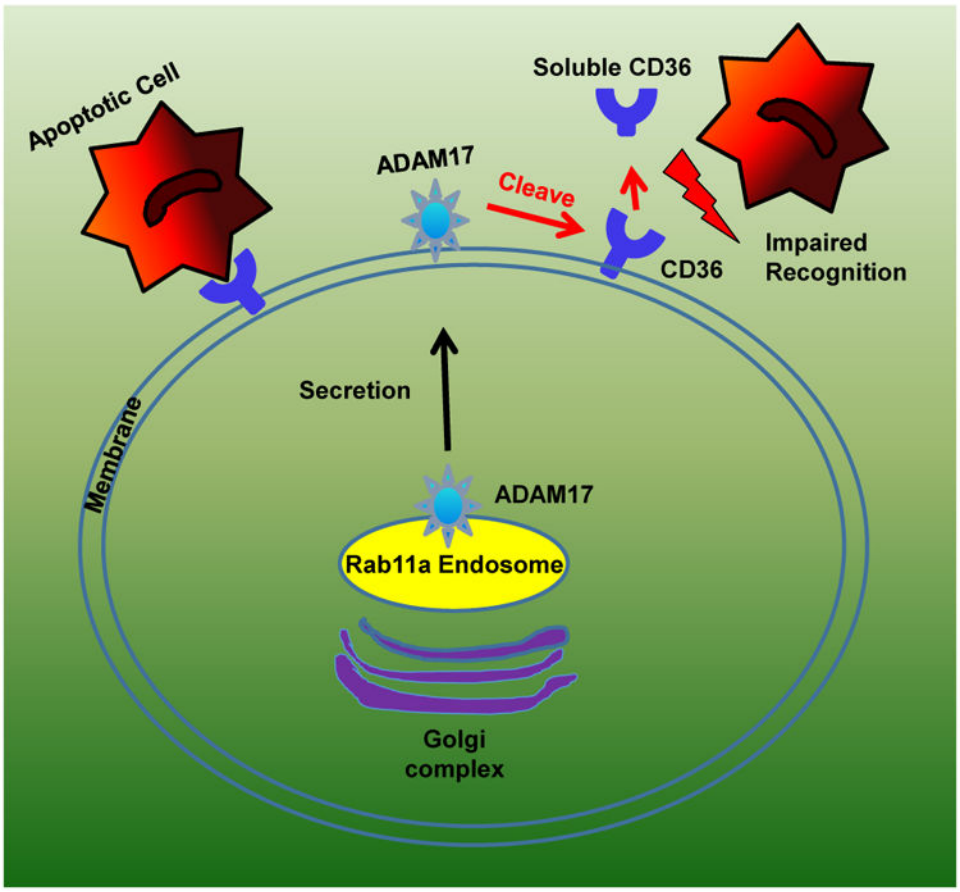

Figure 10. Model of Rab11a in regulating of phagocytosis of apoptotic PMNs